

Comparison between satellite and instrumental solar irradiance data at the city of Athens, Greece (1)

EGU General Assembly 2015, Vienna, Austria, 12-17 April 2015

Session ERE3.8/HS5.6: Harnessing the resources offered by sun, wind and water: control and optimization

Konstantinou C., Dimoulas A., Sarantopoulos V., Skarlatou E., Pipini M.-I., Atalioti A., Kontini A., Tzouka K., Markonis Y. and D. Koutsoyiannis

Department of Water Resources and Environmental Engineering, National Technical University of Athens, Greece

1. Abstract

In this study, we examine and compare the statistical properties of satellite and instrumental solar irradiance data at the capital of Greece, Athens. Our aim is to determine whether satellite data are sufficient for the requirements of solar energy modelling applications. To this end we estimate the corresponding probability density functions, the auto-correlation functions and the parameters of some fitted simple stochastic models. Finally, we examine whether solar irradiance non-seasonal component exhibits Hurst-Kolmogorov behaviour.

Acknowledgements: This research is conducted within the frame of the undergraduate course "Stochastic Methods in Water Resources" of the National Technical University of Athens (NTUA). The School of Civil Engineering of NTUA provided moral support for the participation of the students in the Assembly.

In addition, K. Tzouka, Y. Markonis and D. Koutsoyiannis would like to acknowledge that they have been financed by the European Union (European Social Fund – ESF) and Greek national funds through the Operational Program "Education and Lifelong Learning" of the National Strategic Reference Framework (NSRF) – Research Funding Program: ARISTEIA II: Reinforcement of the interdisciplinary and/ or inter-institutional research and innovation (**CRESENDO project**; grant number 5145).

2. Instrumental data set

- The ground instrumental data set used was provided by the Hydrological Observatory of Athens (hoa.ntua.gr).
- The instrumental network contains 12 stations with solar irradiation data located at the city of Athens and nearby Attica area (mean altitude at 213m, with only one station above 500m).
- Raw measurements have a 10-minute step and covered the period 2005 – 2015.
- It is regarded as a robust data set (missing values close to zero).
- All measurements are presented in W/m^2 units.

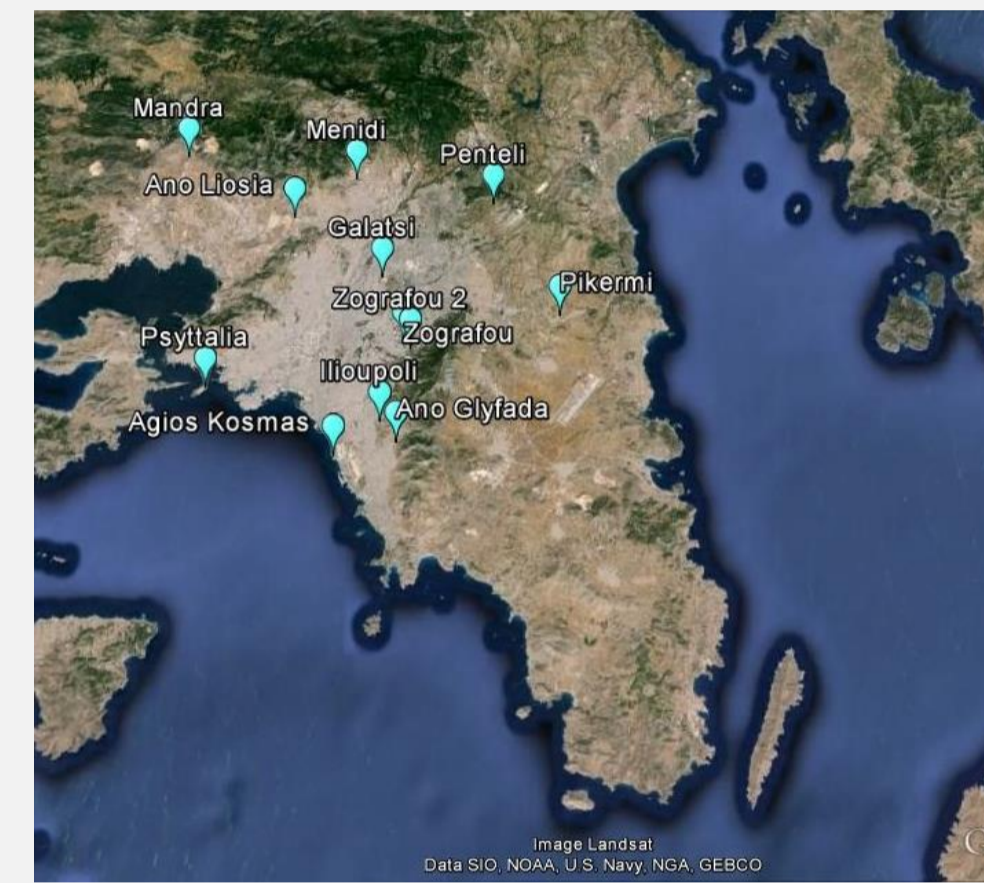


Figure 2.1 Map of the study area

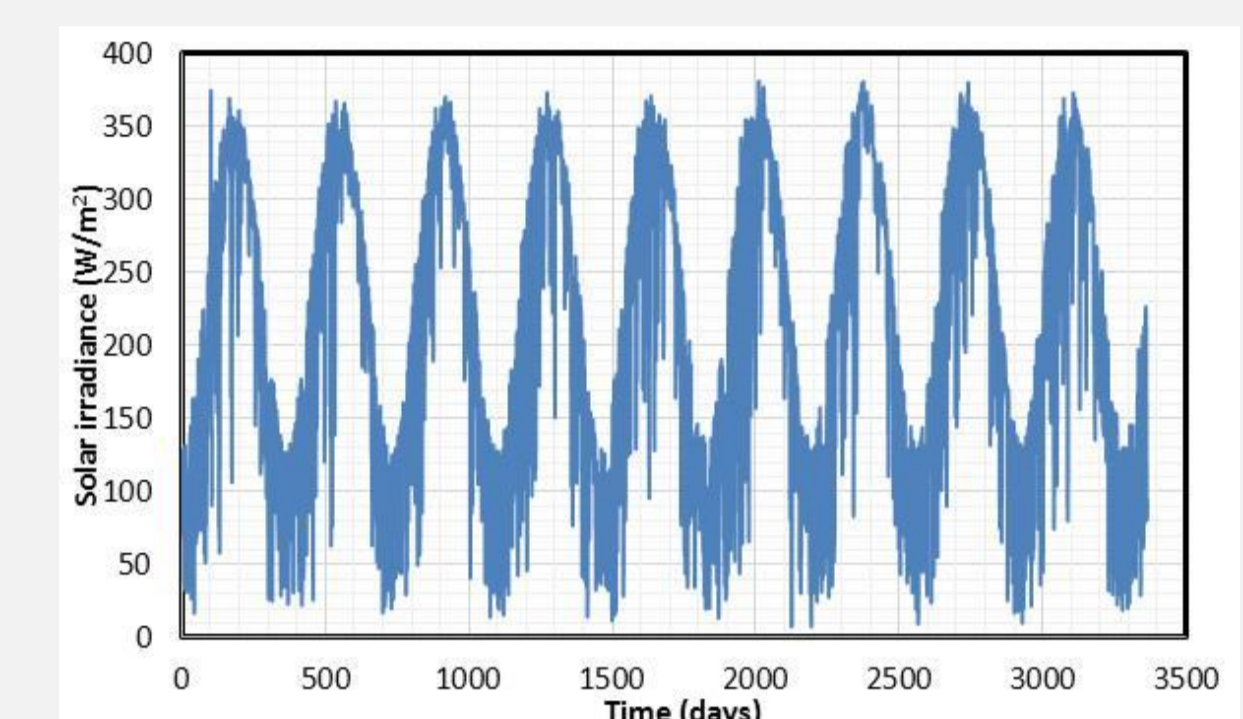


Figure 2.2 Sample daily values of solar radiation (Pikermi station)

3. Satellite data set

- The satellite data set used was provided by the NASA Atmospheric Science Data Center Surface - Meteorology and Solar Energy Division (eosweb.larc.nasa.gov).
- We used a single time series covering the region 38-39 N, 23-24 E with an average altitude of 185m.
- Raw data had daily time step, covering the period between 1983 and 2005 (there is no overlapping with instrumental data) and $KWhr/m^2$ units.
- As it can be seen in Figure 3.1, the satellite grid cell (slashed red line rectangle) does not cover the whole instrumental area (orange line circle). However, we chose to use only one grid cell in order to avoid any reduction of the variance due to aggregation.
- The rate of change of solar irradiance as the latitude increases (Figure 3.2) implies that the instrumental data are expected to yield higher values than the satellite. Notably, the 37-38 and 38-39 cells are both below the regression line.



Figure 3.1 Comparison of satellite grid cell and station network

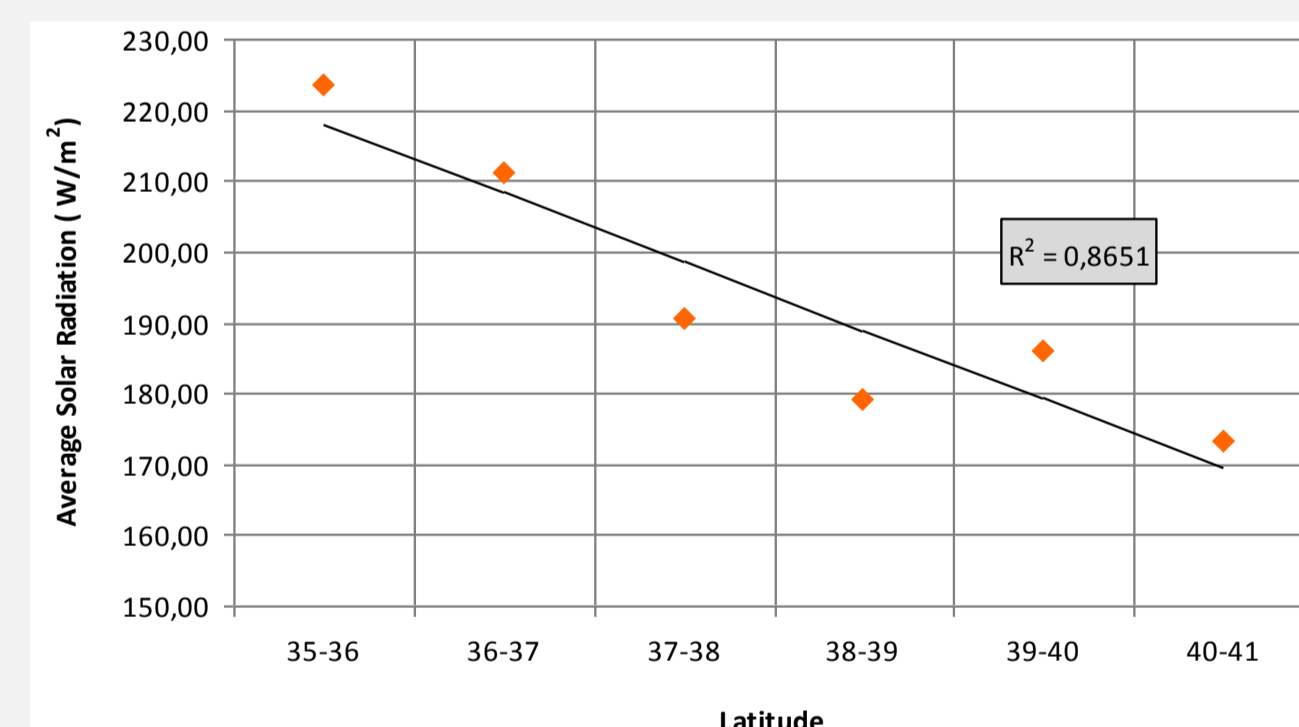


Figure 3.2 Mean irradiance (measured by the satellite) versus latitude

4. Methodology

Our approach to compare ground instrumental and satellite data can be outlined as:

1. Initial pre-processing of data and aggregation to time scales of interest.
2. Detection and removal of outliers and systematic errors. Merging of any problematic record with a corresponding nearby one as long as they share similar statistical properties at their non-problematic part.
3. Estimation of the statistical properties (first 4 moments) of each data set and their empirical distributions. Determination of linear relationships between the statistical moments for instrumental and satellite data.
4. Removal of the seasonality component and re-estimation of the statistical properties of the time series, along with their auto-correlation functions.
5. Estimation of the Hurst coefficient, in order to determine the existence of Hurst - Kolmogorov behaviour (also known as long-term persistence).

5. Raw data processing

Before any statistical analysis and/or comparison between the two data sets was applied, some initial steps were taken to identify any errors in instrumental data (notably, the time series were already checked by the data provider). To this end, we used the data analysis *Hydrognomon* software (www.hydrognomon.org).

The main steps taken were:

- Aggregation of the initial time step (10 minutes) to hourly with a threshold of 5 missing values per hour (a single 10-min measurement would suffice) and then to a daily step with a threshold of 9 values.
- Outliers were removed based on the $(\mu - 3\sigma, \mu + 3\sigma)$ range, where μ is the sample mean and σ the corresponding standard deviation.
- A time series from the average daily values was created to be used as 'standard' in terms of comparison with each instrumental record.
- Systematic errors were detected after the comparison with the standard time series (such as the station of Zografou 1, shown below).
- Merging of the time series in the stations of Zografou 1 and Zografou 2 to a single time series, after determining that their statistical properties match (for the non-problematic segment).

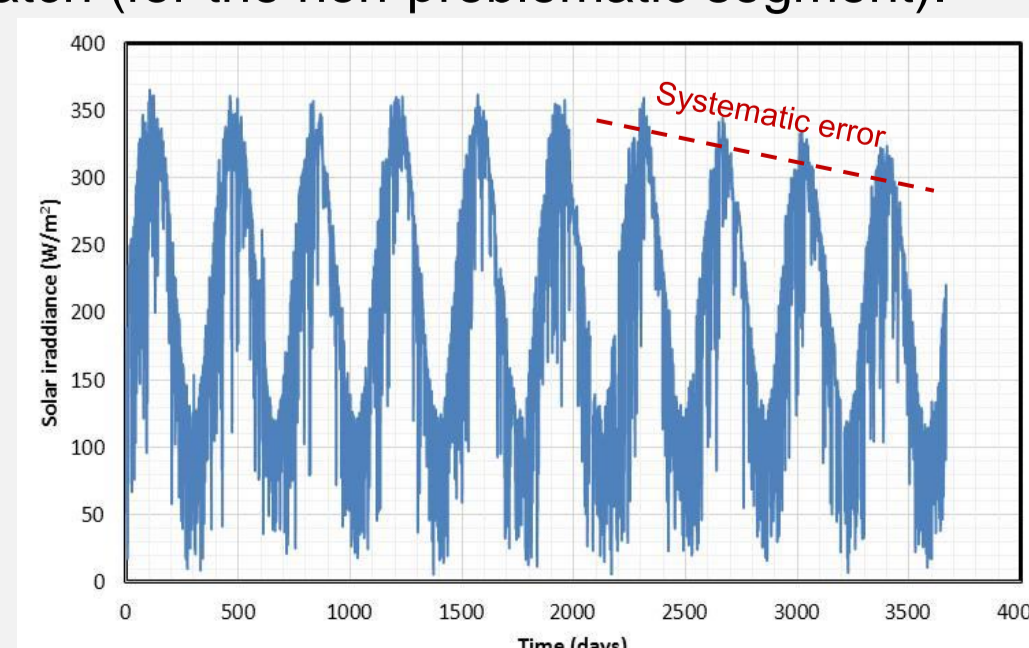


Figure 5.1 Daily values of solar irradiation at the Zografou 1 station.

6. Statistical properties of instrumental and satellite time series (I)

	Month	10	11	12	1	2	3	4	5	6	7	8	9	Mean
Satellite	Mean	127,3	79,2	63,7	79,3	110,8	151,8	216,3	254,4	302,0	293,5	263,1	203,3	178,4
	Stdev	53,9	40,7	34,0	38,9	52,4	70,0	70,0	66,6	46,7	40,1	38,4	46,9	98,4
	Skew	-0,47	-0,03	0,06	-0,05	-0,05	-0,18	-0,53	-1,14	-1,35	-1,29	-0,94	-1,05	0,02
	Kurt	-0,80	-1,19	-1,37	-1,24	-1,12	-1,16	-0,53	0,88	2,76	3,67	1,72	1,01	-3,00
Instrumental	Mean	156,7	109,6	83,3	94,7	124,6	188,7	242,0	280,3	312,3	319,2	292,0	223,2	206,3
	Stdev	50,8	37,8	33,8	36,4	50,9	63,8	65,9	63,9	49,0	31,8	22,6	47,8	96,6
	Skew	-0,80	-0,65	-0,34	-0,29	-0,32	-0,88	-0,97	-1,29	-1,75	-2,19	-1,76	-1,21	-0,16
	Kurt	0,26	-0,35	-1,10	-0,92	-1,04	-0,10	0,24	0,89	3,26	5,74	5,21	1,33	-3,02
Difference	Mean	-29,4	-30,4	-19,6	-15,4	-13,8	-36,9	-25,7	-26,0	-10,4	-25,7	-28,9	-19,9	-27,9
	Stdev	3,1	2,9	0,2	2,5	1,5	6,2	4,2	2,7	-2,3	8,3	15,8	-0,9	1,7
	Skew	0,33	0,62	0,40	0,24	0,27	0,70	0,44	0,15	0,40	0,89	0,82	0,16	0,17
	Kurt	-0,54	-0,84	-0,27	-0,33	-0,08	-1,07	-0,76	-0,02	-0,50	-2,07	-3,50	-0,32	0,02

The comparison between the statistical properties of instrumental and satellite data (table above) shows that:

- The mean of the instrumental data is higher (satellite data are 86.5% of the former).
- The two time series maintain the rest three statistical moments.
- The absolute difference is close to 28 W/m^2 and it ranges between 10 (winter) and 37 W/m^2 (spring).

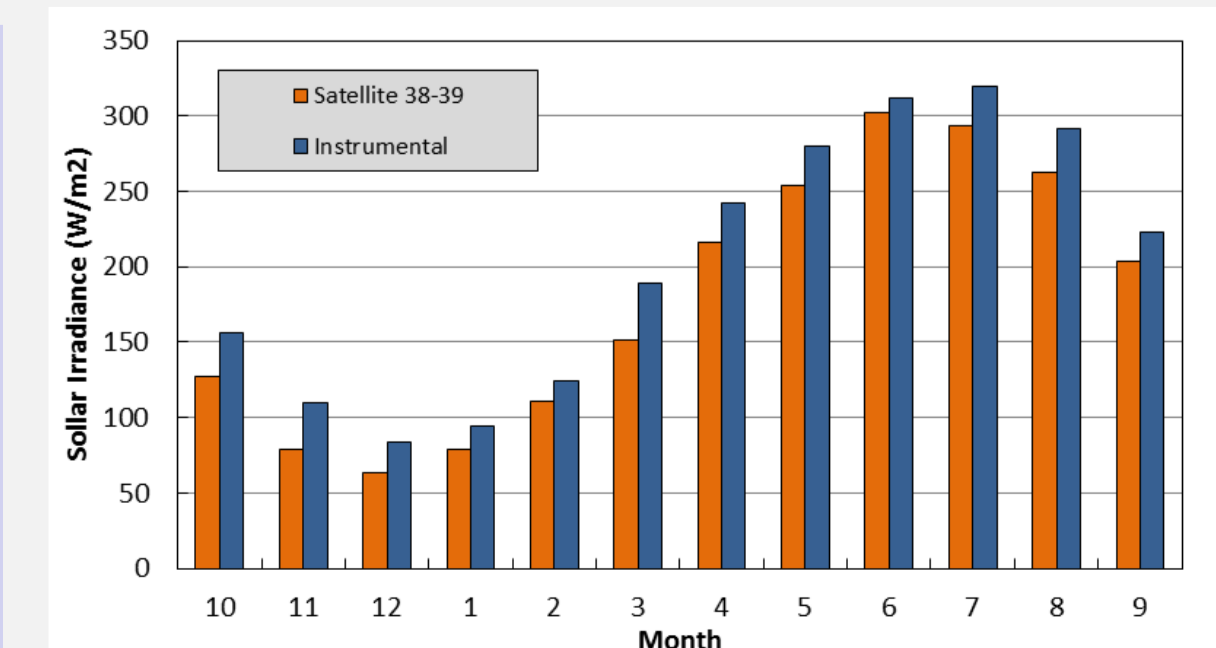


Figure 6.1 Mean monthly values of solar irradiation

Comparison between satellite and instrumental solar irradiance data at the city of Athens, Greece (2)

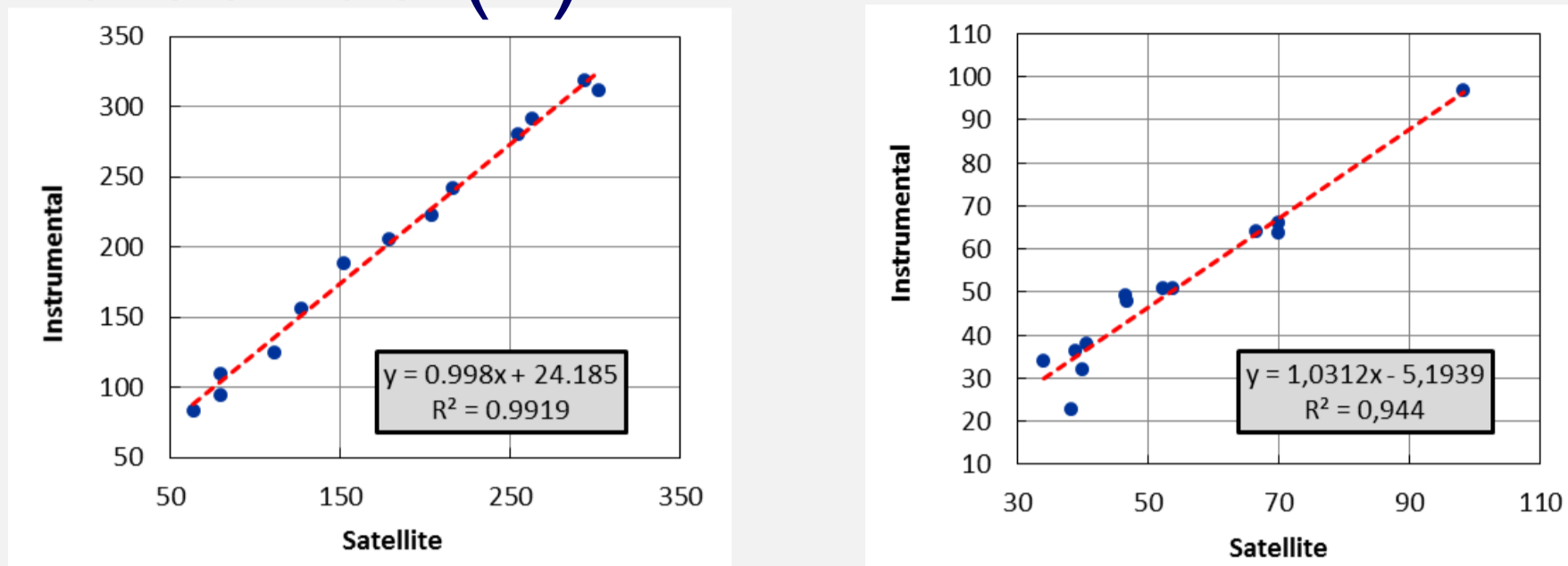
EGU General Assembly 2015, Vienna, Austria, 12-17 April 2015

Session ERE3.8/HS5.6: Harnessing the resources offered by sun, wind and water: control and optimization

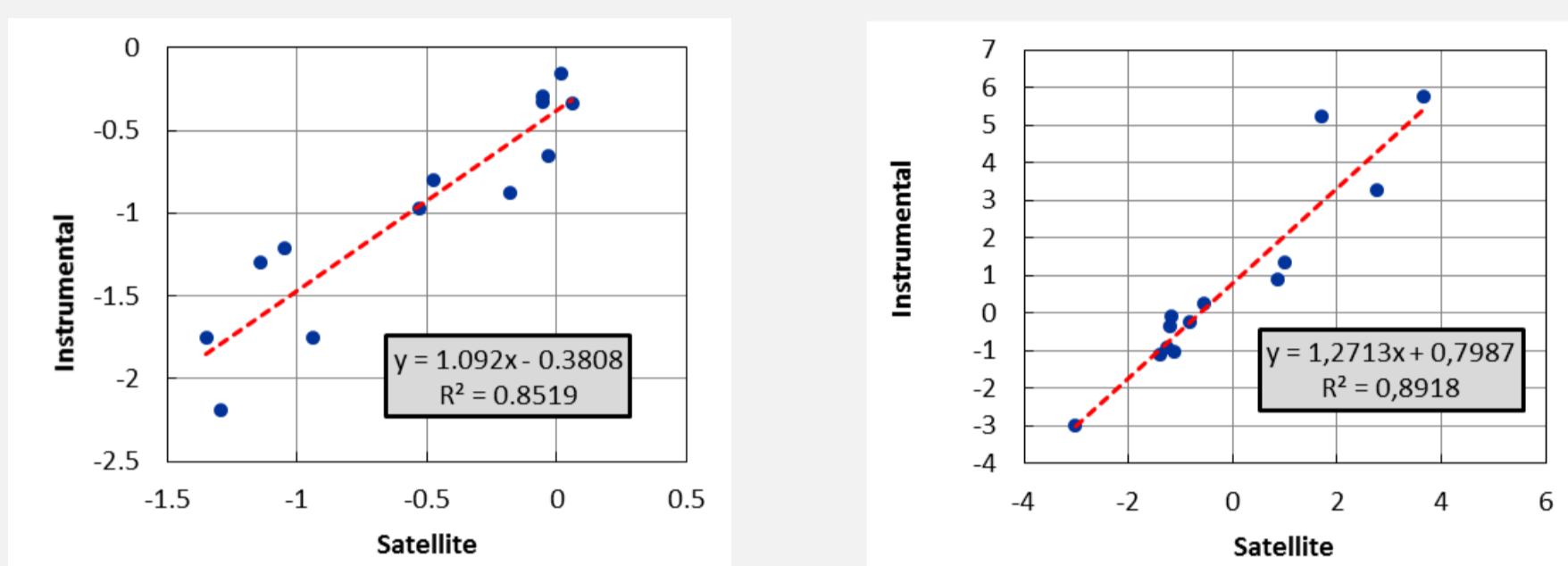
Konstantinou C., Dimoulas A., Sarantopoulos V., Skarlatou E., Pipini M.-I., Atalioti A., Kontini A., Tzouka K., Markonis Y. and D. Koutsoyiannis

Department of Water Resources and Environmental Engineering, National Technical University of Athens, Greece

6. Statistical properties of instrumental and satellite time series (II)



Figures 6.2 & 6.3 Empirical relationships between 1st (left) and 2nd (right) order statistical moments of the monthly values of instrumental and satellite data sets.



Figures 6.4 & 6.5 Empirical relationships between 3rd (left) and 4th (right) order statistical moments of the monthly values of instrumental and satellite data sets.

7. Removal of seasonality component

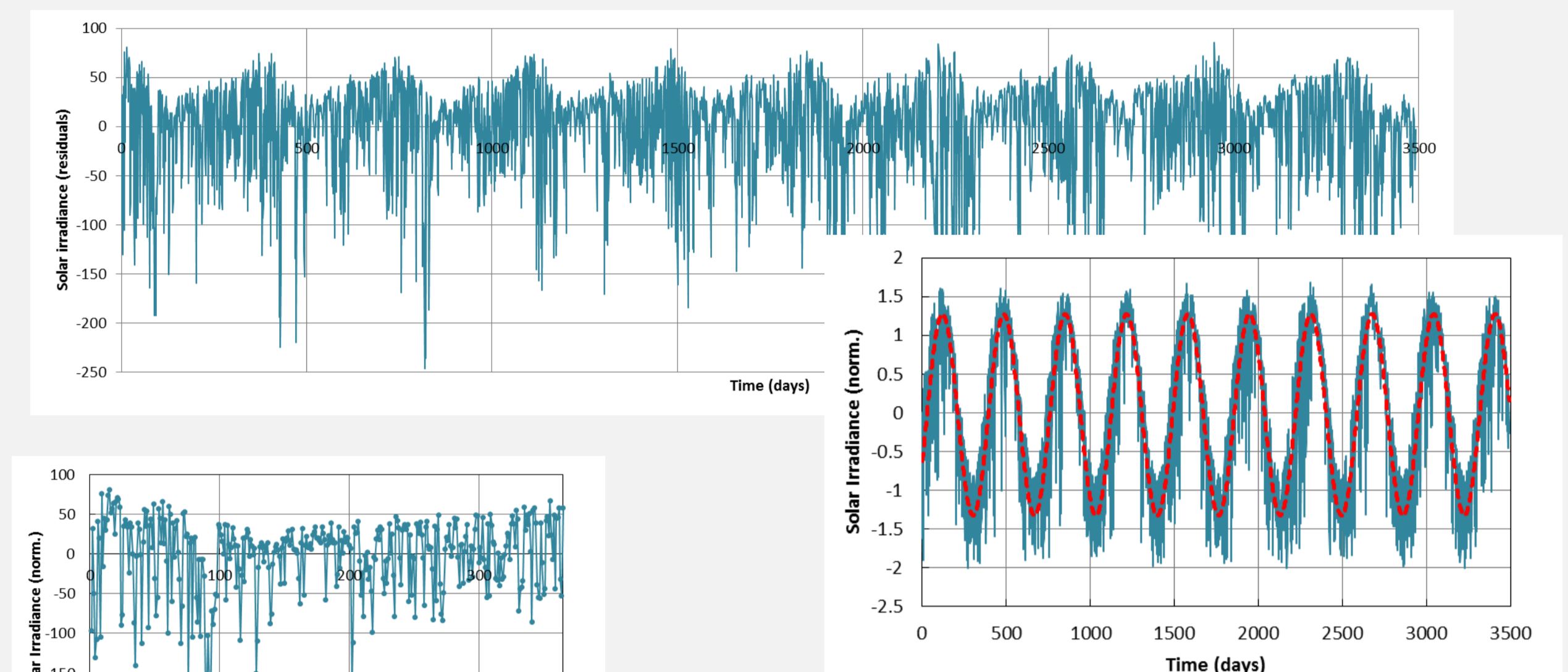


Figure 7.3 Initial time series & fitted sine function

Figures 7.1 & 7.2 Residuals of instrumental data (above) and single year in detail (embedded figure).

The fitting methodology is based on root mean square error (RMSE) minimization between the original time series and the deterministic seasonal component. The sine function which is used is $y = 1.3 \sin(0.017x - 0.5) - 0.025$ for the instrumental data and $y = 1.3 \sin(0.017x - 0.5) - 23.025$ for the satellite data.

8. Autocorrelation functions & empirical distributions

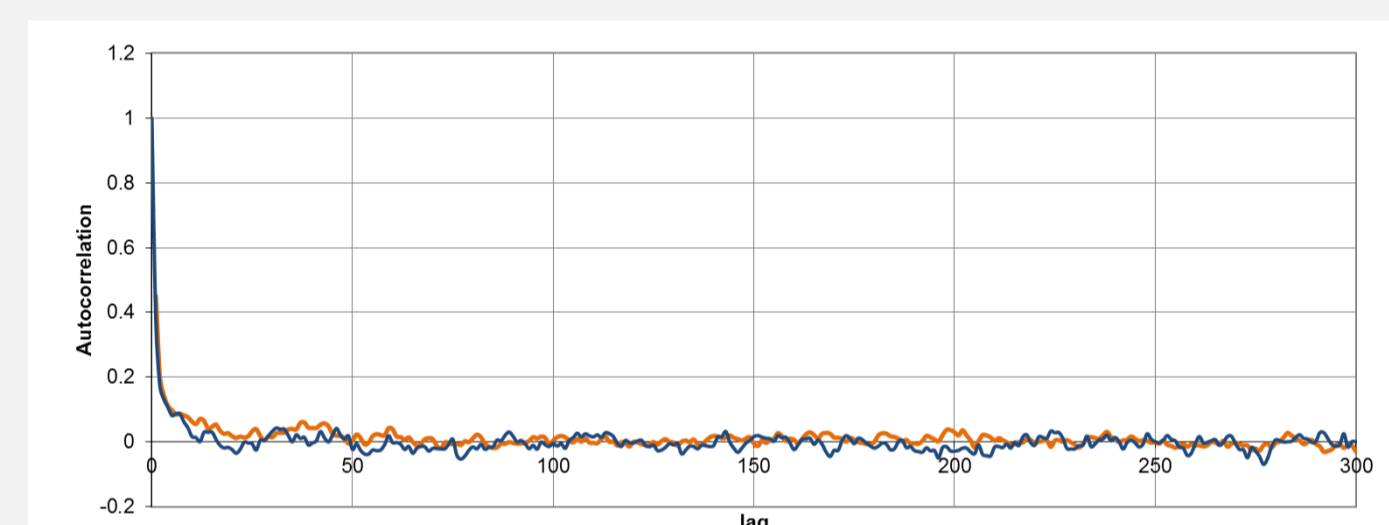


Figure 8.1 Autocorrelation functions (ACFs) of instrumental (orange) and satellite (blue) values

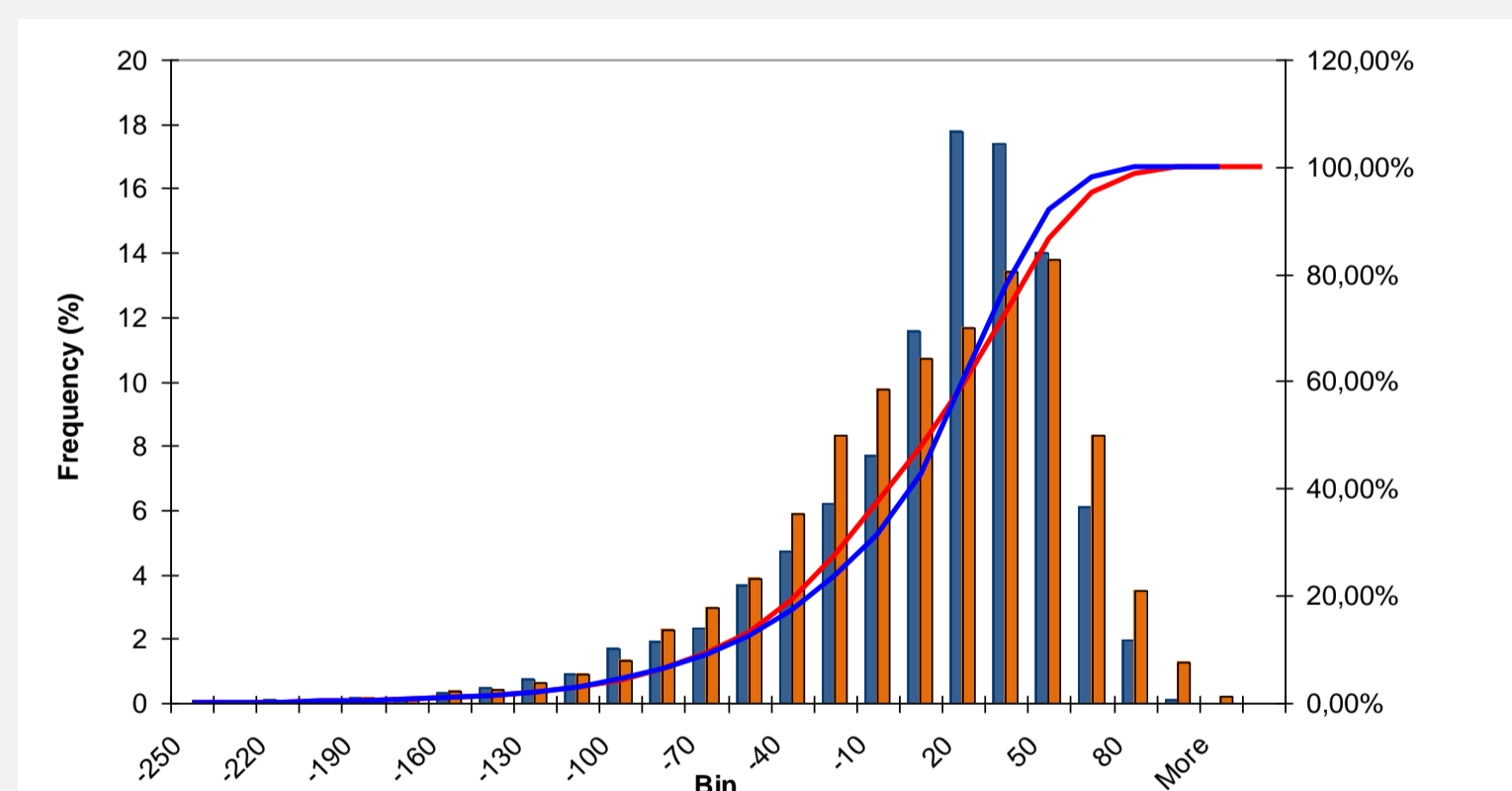
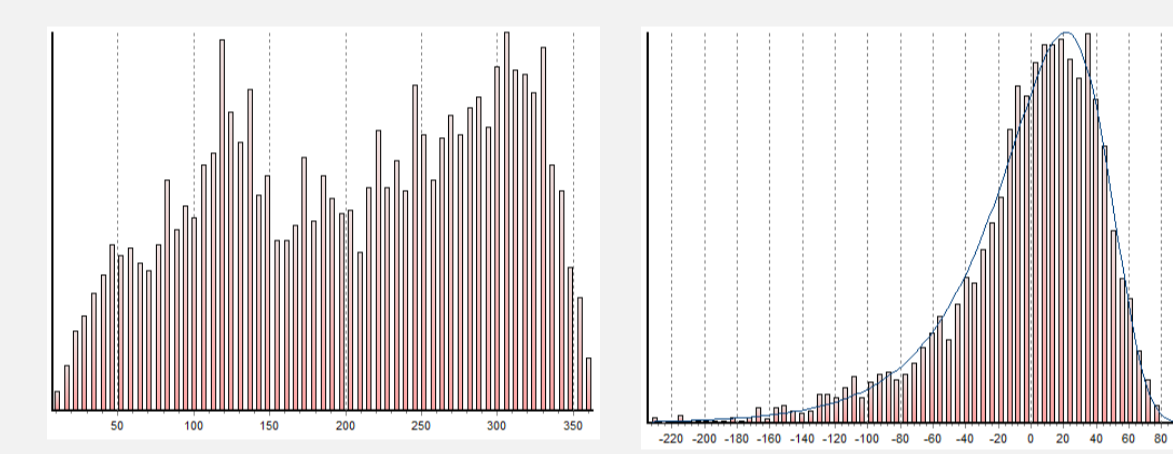


Figure 8.2 Empirical distributions (same colours)

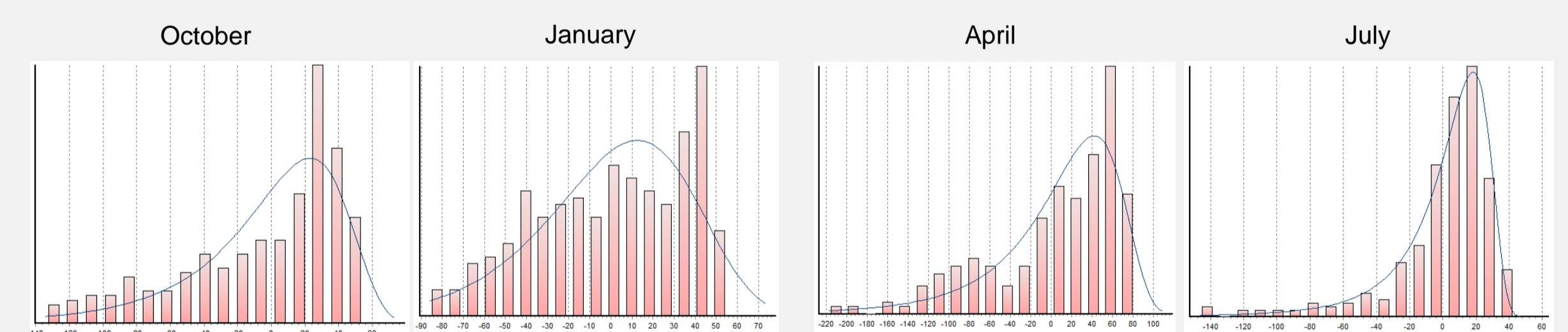
- The ρ for lag 1 is close to 0.4 for both data sets.
- There is an exponential decrease in both instrumental and satellite data sets (non-seasonal components).
- This decrease exhibits the same pattern in both data sets, without any significant deviation.
- These results might imply that a low order auto-regressive, e.g. AR(1), stochastic process is sufficient to describe the observed variability [Beran, 1994].
- The empirical distributions share similar properties, with a minor difference concerning the 20-50 W/m^2 range, where satellite data are higher.
- The skewness of the data is due to summer cloudiness, when the removed seasonal component is higher.

9. Effect of seasonality component removal to the empirical distributions



Figures 9.1 – 9.2 Empirical distributions of mean solar irradiance instrumental time series (averaged over all stations), with seasonal component (left) and when the component is removed (right). Blue line corresponds to a theoretical GEV distribution fitted to data for illustrative purposes, as modelling of the time series lies beyond the scope of this study.

- Removal of the seasonality component, also offers a better opportunity to fit a theoretical distribution to the data (Figures 9.1 and 9.2).
- However, if the corresponding monthly distributions are examined, we can see that only July (and summer months in general) are adequately described by the GEV distribution, which was found to have the best fit.
- Satellite data set gave similar results (not shown here).



Figures 9.3 – 9.6 Monthly empirical distributions of mean non-seasonality component of solar irradiance (averaged over all stations)

10. Hurst coefficient estimation

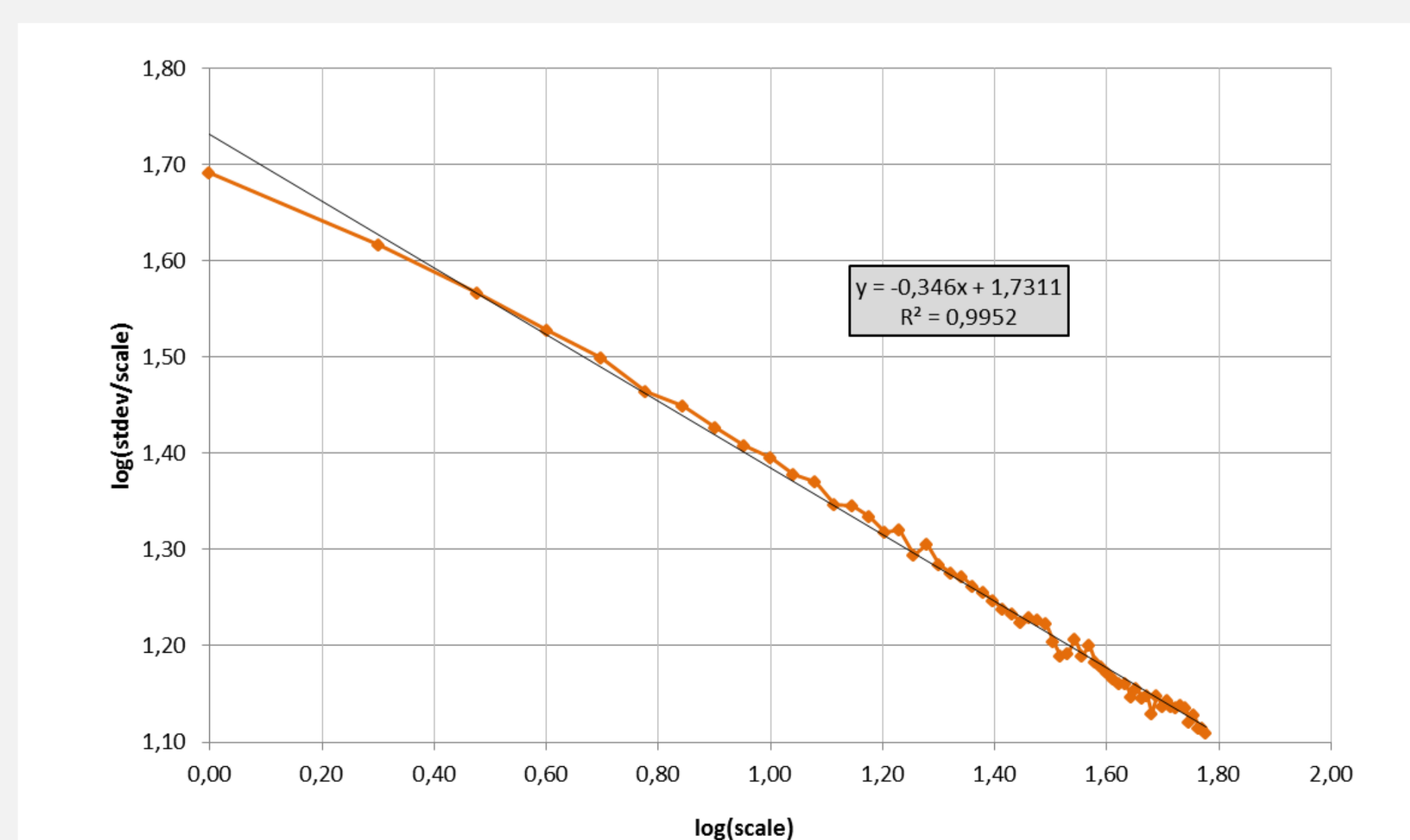


Figure 10.1 Estimation of Hurst coefficient H by climacogram; slope of logarithmic plot of aggregated standard deviation versus scale [Koutsoyiannis, 2002]. $H = 1 + \alpha = 0.65$, where α is the slope. Although, the autocorrelation functions seem to fall exponentially to zero after a few lags (Markovian behaviour), we can see that Hurst-Kolmogorov behaviour is evident. This could be a result of the bias encountered when ACF is used [Dimitriadis and Koutsoyiannis, 2015].

11. Conclusions

1. Initial processing of instrumental data showed that they are high-quality, robust time series with almost inexistent missing gaps. However, their record lengths were only 10 years for the majority of them.
2. Satellite data have longer record length (22 years) for a different chronic period, but they lack in resolution ($1^\circ \times 1^\circ$).
3. The comparison between instrumental and satellite data showed that their mean values deviate for $28 W/m^2$ (instrumental are higher). The difference remains throughout the year and is higher for the summer season.
4. There are strong linear relationships ($R^2 > 0.85$) between the statistical moments of both data sets. Therefore, we are able to combine them to a single, longer record. Their ACFs also agree with that (with little discrepancies).
5. The removal of seasonality highlighted another cycle considering the variance, which increases during the winter months (due to cloudiness).
6. We have found evidence of Hurst-Kolmogorov behaviour, even though the autocorrelogram results could be interpreted as a Markovian-type behaviour.

References

- Beran, J. (1994). *Statistics for long-memory processes* (Vol. 61). CRC Press.
- Dimitriadis, P., & Koutsoyiannis, D. (2015). Climacogram versus autocovariance and power spectrum in stochastic modelling for Markovian and Hurst-Kolmogorov processes. *Stochastic Environmental Research and Risk Assessment*, 1-21.
- Koutsoyiannis, D. (2002). The Hurst phenomenon and fractional Gaussian noise made easy. *Hydrological Sciences Journal*, 47(4), 573-595.